THE ASTROPHYSICAL JOURNAL, 380:L71–L74, 1991 October 20

GALACTIC CENTER GASDYNAMICS: A ONE-ARMED SPIRAL IN A KEPLERIAN DISK

J. H. LACY AND J. M. ACHTERMANN[1]
Department of Astronomy, University of Texas, Austin, TX 78712
AND
E. SERABYN[1]
California Institute of Technology, Pasadena, CA 91125
Received 1991 June 3; accepted 1991 August 6

ABSTRACT

The inner 3×4 pc of the Galaxy have been imaged in the [Ne II] (12.8 μm) line with 2″ and 30 km s^{-1} resolution. The morphology of much of the ionized gas can be explained by a one-armed linear ($r \propto \theta$) spiral. The kinematics of the gas along the spiral can be modeled by approximately circular orbits with a nearly Keplerian rotation curve, requiring a central mass of $2 \pm 0.5 \times 10^6\ M_\odot$. Several possible origins are suggested for the spiral.

Subject headings: black holes — galaxies: nuclei — galaxies: The Galaxy — infrared: spectra

1. INTRODUCTION

At the center of the Milky Way lies a complex region of stars, gas, and dust of confusing morphology and kinematics (see, e.g., Genzel & Townes 1987 and Morris 1989). The most controversial question about this region concerns the existence of a massive black hole, a possibility first suggested by Lynden-Bell & Rees (1971). The first kinematic evidence was obtained by Lacy et al. (1980); subsequent observations of the ionized gas kinematics (e.g., Serabyn & Lacy 1985) have supported this suggestion, but with persistent questions about the three-dimensional morphology of the gas and the possible influence of nongravitational forces (e.g., Lacy 1989). Observations of stellar kinematics, with different systematic uncertainties, give additional, but still not convincing, evidence of a massive central object (Rieke & Rieke 1988; Sellgren et al. 1990).

The central few parsecs of the Galaxy can be divided into two regions. Outside of ~1.5 pc radius,[2] the gas is predominantly molecular and organized into a disklike structure. The rotation curve of the disk is approximately flat, with an orbital speed of ~110 km s^{-1} (Serabyn et al. 1986; Güsten et al. 1987; Sutton et al. 1990). Inside of 1.5 pc, the most prominent gas is ionized. The ionized gas (Sgr A West) is organized into a number of streamers or filaments (Lo & Claussen 1983), several of which have been named; the "western arc," "northern arm," "eastern arm," and "bar" are identified in Figure 1. Near the center of Sgr A West lies a unique nonthermal radio source, Sgr A* (see Lo 1989), which is thought to lie at or near the center of the nuclear mass distribution. Serabyn & Lacy (1985) and Serabyn et al. (1988) measured [Ne II] (12.8 μm) spectra from many locations along the streamers and found organized patterns of velocities. They interpreted the western arc as the ionized inner edge of the molecular disk in an approximately circular orbit with an orbital speed of ~110 km s^{-1} and modeled the northern arm as a tidally stretched cloud following an eccentric orbit passing ~0.4 pc behind the center. Radio recombination line observations (Schwartz, Bregman, & van Gorkom 1989; Roberts et al. 1991), confirm the velocity pattern seen in [Ne II].

In this *Letter*, we discuss new observations of [Ne II] emission from the ionized gas in the inner few parsecs of the Galaxy. These observations lead us to consider a new interpretation of the morphology of much of the ionized gas, which allows a more coherent interpretation of the kinematic data, thus strengthening the argument for a massive black hole.

2. OBSERVATIONS

Observations of [Ne II] (12.8 μm) emission from Sgr A West were made on 1989 July 28 with Irshell, a mid-infrared cryogenic echelle spectrograph (Lacy et al. 1989), on the NASA IRTF. Irshell uses a 10×64 pixel Si:As detector array to measure a 64 point spectrum at each of 10 positions spaced by 1″ in the sky. The spectral dispersion was 0.043 cm^{-1}, or 16.5 km s^{-1}, per pixel, and the resolution was about 2 pixels FWHM. For mapping the Galactic center, the IRTF chopping secondary was not driven. Instead, the telescope was scanned repetitively across the source. The sky background was determined for each pixel of the detector array from the lowest region of each scan. An area of 75″ × 90″ was mapped with 0.″6 × 1.″0 sampling and 2″ resolution.

A [Ne II] line map was constructed from the data cube by summing the channels covering Doppler shifts from +380 to −412 km s^{-1}, and subtracting the continuum emission, determined from channels covering −412 to −648 km s^{-1}. The map is shown in Figures 1 and 2*a* (Plate L4). It is nearly identical to VLA maps of free-free emission (see Fig. 3 [Pl. L5]), demonstrating that Ne II] is a good tracer of ionized gas. The complete data cube will be presented in a future paper.

3. MORPHOLOGY

Several authors have suggested that there may be connections between the various ionized filaments in Sgr A West (Lo & Claussen 1983; Quinn & Sussman 1985; Serabyn et al. 1988), but the available data did not make these connections entirely convincing. Our new observations lead us to reconsider this idea. In particular, a bridge of emission can be seen between the western arc and the northern arm below IRS 8,

[1] Visiting Astronomer at the Infrared Telescope Facility, which is operated by the University of Hawaii under contract from the National Aeronautics and Space Administration.

[2] We assume 1 pc = 25″, or $R_\odot = 8.5$ kpc.

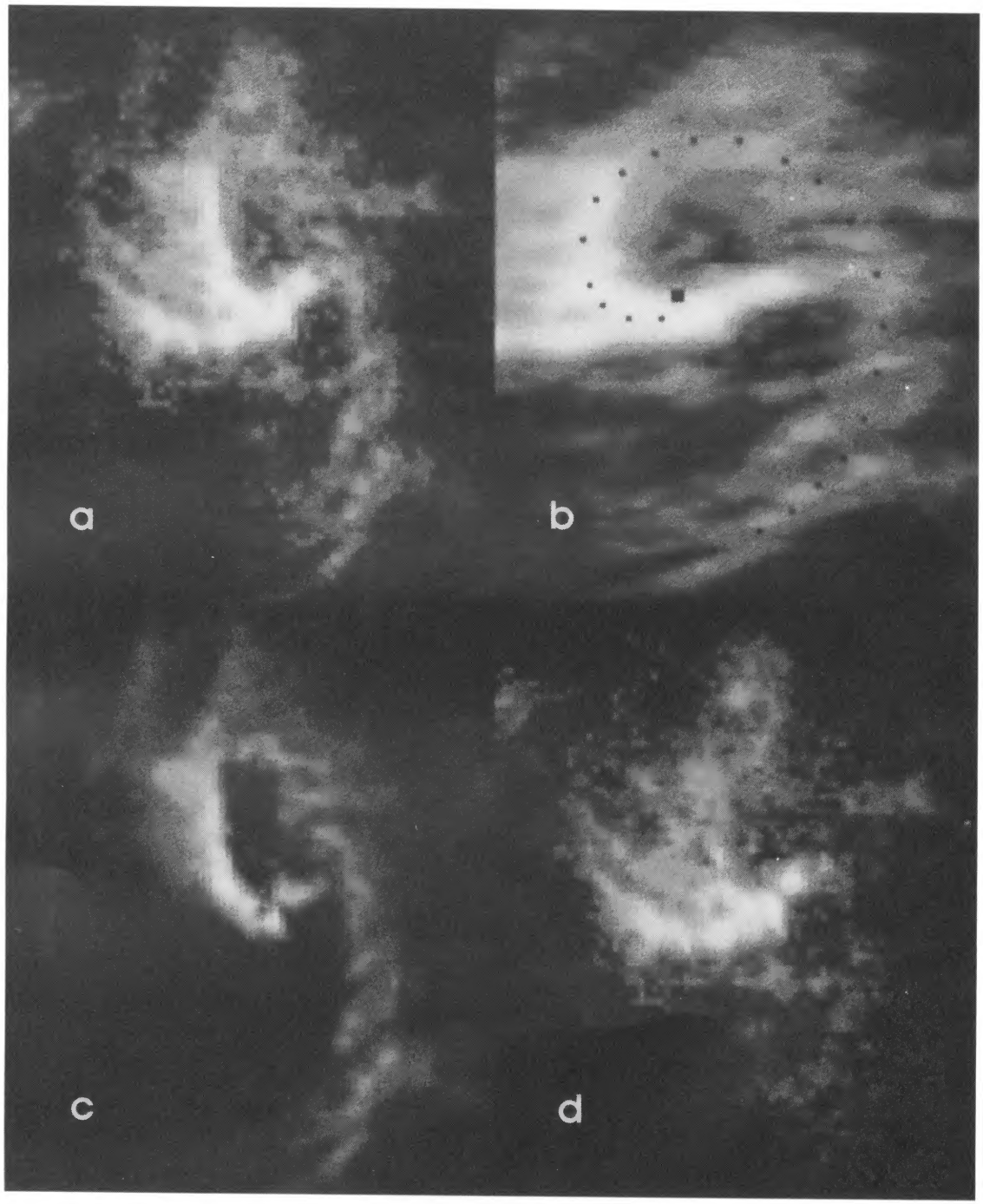

FIG. 2.—(*a*) Image of [Ne II] emission from Sgr A West. A logarithmic brightness transfer function was used. (*b*) Image of [Ne II] stretched to correct for the projection of the spiral plane onto the plane of the sky. The fitted spiral is traced out with black pixels. Note that the features not in the spiral may not be correctly deprojected. (*c*) Image of [Ne II] including only a velocity range of ± 40 km s^{-1} about the velocity expected at each point in a Keplerian disk. (*d*) Image of [Ne II] excluding the gas with the disk velocity pattern.

LACY, ACHTERMANN, & SERABYN (see 380, L71)

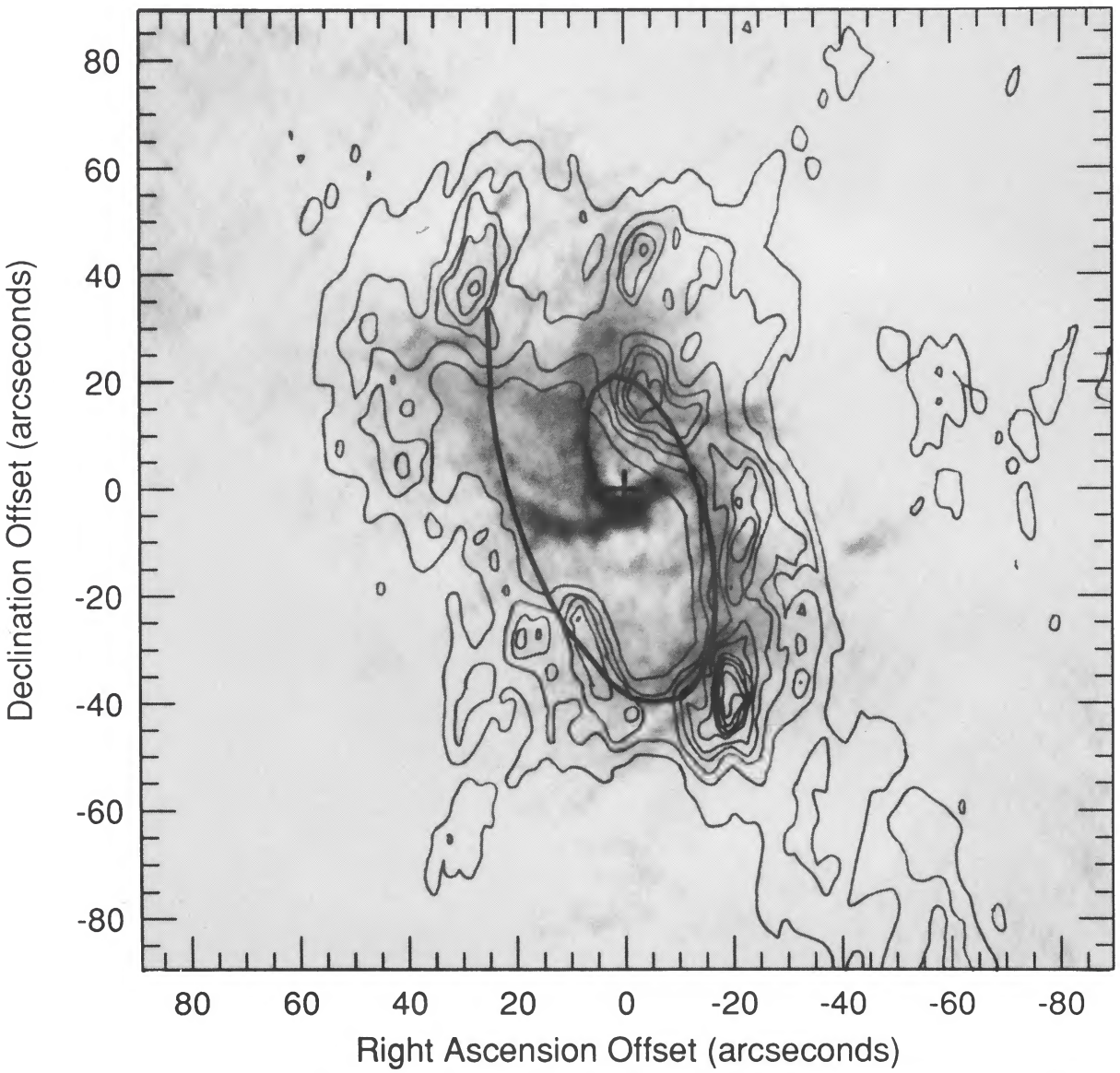

FIG. 3.—Contour map of HCN $J = 1$–0 emission from Wright et al. (1987) superposed on gray-scale representation of the 5 GHz free-free emission from Lo & Claussen (1983). The spiral which fits the [Ne II] observations is shown, extrapolated beyond the ionized gas region. The HCN emission peaks outside of this spiral.

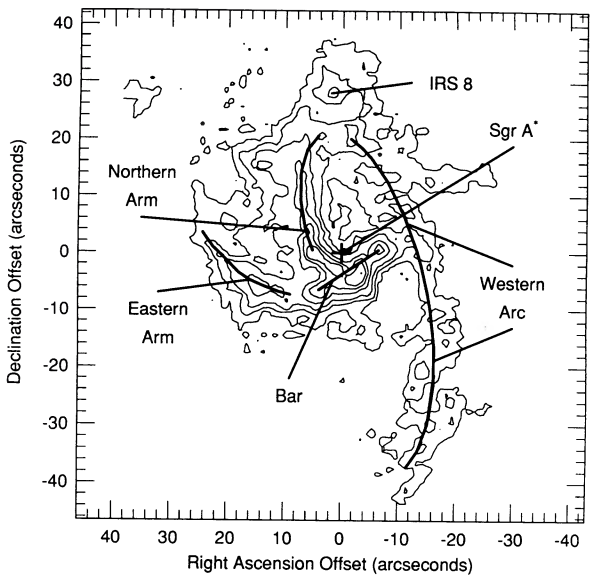

FIG. 1.—Contour map of [Ne II] (12.8 μm) emission from Sgr A West, with features discussed in the text identified. Contour levels are (3, 6, 10, 20, 30, 40, 60) $\times 10^{-2}$ ergs s^{-1} cm^{-2} sr^{-1}. Noise level (1 σ) is 0.7 $\times 10^{-2}$.

and there seems to be a continuation of the northern arm into the bar, ending $\sim 2''$ south of Sgr A*. A connection between the western arc and the northern arm is supported by kinetic models which place them, and the molecular disk, in nearly the same planes. Serabyn & Lacy (1985) fitted the northern arm as a streamer orbiting in a plane with an inclination of $i = 60°$–$70°$ from face-on and a position angle of intersection with the sky plane of p.a. $\approx 20°$. For the western arc plane, they find $i = 60°$–$70°$ and p.a. $\approx 12°$. Published numbers for the molecular disk range over $i = 60°$–$70°$ and p.a. $= 0°$–$30°$ (Serabyn et al. 1986; Güsten et al.; Sutton et al.).

The face-on appearance of gas in an inclined plane can be determined by stretching the observed image. The stretched, or deprojected, [Ne II] image, assuming $i = 65°$ and p.a. $= 15°$, is shown in Figure 2*b*. Two new conclusions are suggested by this image. First, the western arc is not well described by a circle centered near Sgr A*; instead, it appears to follow an offset circle or spiral (see also Mezger & Wink 1986), separated from Sgr A* by $\sim 20''$ at the top of the image and $\sim 40''$ at the bottom. Second, the combined western arc and northern arm trace out an approximately linear spiral, with $r \propto (\theta - \theta_0)$, where θ is the angular coordinate in the deprojected plane, relative to the line of intersection of the plane with the plane of the sky.

To obtain a more quantitative idea of how well a spiral fits these features, we used a least-squares fitting routine (GaussFit; Jefferys, McArthur, & McCartney 1990) to simultaneously determine the position angle and inclination of the plane of the spiral, the location of the center, and the variation of r with θ, by fitting the positions of [Ne II] emission peaks along the spiral. A cubic polynomial was assumed for $r(\theta)$, but the quadratic and cubic terms were found to be consistent with zero, so dropped. The best-fitting linear spiral is traced by black dots in Figure 2*b*. (Portions of the spiral, projected onto the plane of the sky, form the curves labeled "western arc" and "northern arm" in Fig. 1.) The derived parameters are p.a. $= 15° \pm 2°$, $i = 65° \pm 5°$, $\theta_0 = 187° \pm 10°$, and $dr/d\theta = -0.25 \pm 0.05$ pc rad^{-1} (1.6 pc/360°). The best center position was 1″ north of Sgr A*, with an uncertainty of $\sim 1''$. All uncertainties are estimated from variations in derived parameters when questionable points were excluded from the fit. The spiral is apparent in ionized gas over the range $\theta \approx -180$ to $+180°$.

Several prominent emission features do not fit into the spiral pattern. These include much of the bar, the eastern arm, the ionized gas to the east of the northern arm, and IRS 8. These features also do not fit the velocity pattern discussed below. In addition, the fitted spiral deviates noticeably from the narrow ridge of emission just southeast of Sgr A*.

Since the western arc follows closely the ridge of bright HCN emission along the inner edge of the molecular disk, one might expect the spiral derived from the [Ne II] data to continue to follow features in the molecular emission beyond the region where ionized gas is seen. In Figure 3 we show the derived spiral superposed on a map of HCN emission (Wright et al. 1987), with the 5 GHz continuum map of Lo & Claussen shown in gray. The spiral follows the inner edge of the HCN emission along the western arc and for $\sim 90°$ beyond the southern end of the western arc, although it lies substantially inside the HCN emission to the northeast. A spiral with a slightly larger pitch ($dr/d\theta \approx -0.3$) would fit most of the HCN emission over $\theta = 0°$ to $-360°$ ($r = 1$–3 pc).

4. KINEMATICS

If the spiral pattern seen in the ionized gas is not a chance superposition of unrelated features, there should be a smooth variation in velocity along its length. To determine the velocity field, we extracted spectra along the spiral from a smoothed version of our data cube and display them as an angle-velocity (θ-v) contour plot in Figure 4. The velocity pattern appears

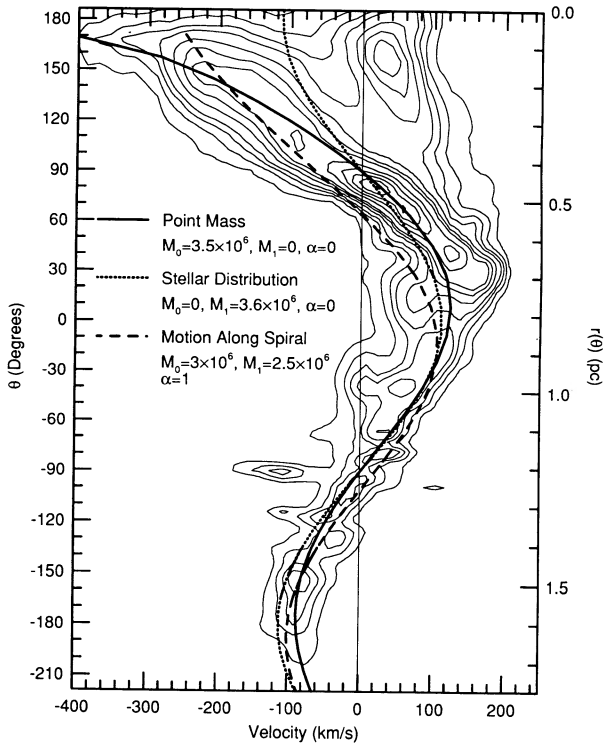

FIG. 4.—[Ne II] spectra along the spiral feature, plotted as a θ-v contour diagram. Three fits to the data are superposed: circular motion in the potential of a point mass (*solid curve*), circular motion in the potential of a singular isothermal star cluster (*dotted curve*), and motion along the spiral in the potential of both stars and a central object (*dashed curve*).

continuous. Although the pattern could be described either as two roughly linear segments meeting at $\theta \approx 30°$ or as a sine wave with an amplitude increasing toward the center, the continuity in both position and velocity suggests that they form a single feature. The sinusoidal Doppler pattern would then be ascribed to the projection of approximately circular velocities onto the line of sight, and the variation in amplitude would indicate an orbital speed rising toward the center. Most of the emission along the spiral fits into this pattern, although a few discrepant velocities are seen (between 120° and 180° and near −90°, where the spiral crosses the bar).

In order to determine the dependence of the gas velocity on distance from the center, we fitted the observed Doppler shifts of peaks along the spiral, assuming the motion is in the plane of the fitted spiral. Anticipating an interpretation of the velocities as orbital motion in a gravitational potential, we parameterized the variation of the angular component of velocity with radius, r, as $v_\theta = [GM(r)/r]^{1/2}$, with $M(r) = M_0 + M_1 r$, where M_0 is the central mass and M_1 is the stellar mass per parsec, assuming a singular isothermal cluster (and neglecting the perturbation of the stellar distribution caused by the central mass). We first assumed that the motion is along the spiral [$v_r = v_\theta \tan(\theta_{\rm pitch})$] but found a systematic disagreement between the data and the best fitting model in the sense that the fitted θ-v curve was shifted in θ from the data (see Fig. 4). We next tried varying the spiral orientation and rotation curve simultaneously, but found a poor spatial fit when the position angle of the plane was varied to give a good kinematic fit. The disagreement suggested that v_r is less than assumed. As a simple way of allowing different radial motions, we then tried multiplying the radial component of the velocity by α, an additional free parameter [$v_r = \alpha v_r$(spiral)]. An acceptable fit was found, with $M_0 = (2.4 \pm 1.0) \times 10^6\ M_\odot$, $M_1 = (1.0 \pm 1.0) \times 10^6\ M_\odot\ {\rm pc}^{-1}$, and $\alpha = -0.2 \pm 0.4$. Of these three parameters, only M_0 is significantly different from zero; the observations do not extend to large enough radius to constrain M_1, and the radial motion is small compared to the circular motion. Several fitted θ-v curves are shown superposed on the data in Figure 4. The curve for the best-fitting case is essentially the same as the solid curve. Although not perfect, the fit is significantly better than for the other cases considered. The curve for motion along the spiral ($\alpha = 1$) is shifted in θ from the data, and the curve for orbits in a star cluster ($M_0 = 0$) does not show the observed variation of the amplitude of the sine wave. Since observations of the molecular ring and stellar velocities constrain M_1 to be approximately $2.5 \times 10^6\ M_\odot\ {\rm pc}^{-1}$, we also fitted the [Ne II] observations assuming this value M_1; M_0 was then $(1.9 \pm 0.5) \times 10^6\ M_\odot$.

Having determined the rotation pattern of the gas in the spiral, we can use the Doppler shifts over our entire map to ask whether other gas could be in the same rotating disk. In Figure 2*c*, we display a [Ne II] image including only the gas with Doppler shifts which fit a projected Keplerian rotation pattern. Except for emission associated with IRS 2 and IRS 6 in the bar, only the spiral is apparent, indicating that the features not in the spiral are also not in the disk. In Figure 2*d*, we display the difference between the images in Figures 2*a* and 2*c*, showing these features.

In conclusion, we find that almost all of the gas along the spiral feature has a velocity pattern consistent with circular motion in a Keplerian disk centered on Sgr A*, and conversely, almost all of the ionized gas with velocities of a Keplerian disk lies along the spiral. In our previous work (e.g., Serabyn & Lacy 1985), we assumed gas motion along the streamers, and by including noncircular motions were able to fit restricted regions of the spiral as several separate features. By dropping the assumption of motion along the features, we now find that the entire spiral can be fitted as a single feature, but only if the motion is nearly circular.

5. ORIGIN OF THE SPIRAL

The models most often considered to explain the gas morphology and kinematics in the Galactic center involve tidally stretched gas clouds (e.g., Serabyn & Lacy 1985; Quinn & Sussman 1985). Serabyn et al. argue that the gas in a tidally stretched cloud would move along the streamer, a possibility our new kinematic measurements rule out for the entire spiral. However, Quinn & Sussman describe a model in which an initially spherical gas cloud, moving through a medium causing drag, is sheared into a spiral with a spatial and Doppler pattern much like that which we see. The cloudlets in their model move on paths intermediate between circular orbits and the path traced by the spiral. The essential differences from the models of Serabyn et al., in addition to the presence of drag, appear to involve the initial conditions assumed.

In order to better understand Quinn & Sussman's models, we repeated their calculations, assuming variously shaped clouds initially orbiting on approximately circular orbits near the inner edge of the molecular disk ($r \approx 1.5$ pc). Several models gave acceptable fits to our observations (which require a spiral with one wrap between $r = 0$ and 1.5 pc and motion more nearly circular than along the spiral). It appears that the requirements for acceptable models are: a drag-producing medium with a density rising rapidly toward the center ($p \propto r^{-3}$ to r^{-6}), a cloud with substantial initial extent ($\gtrsim 0.2$ pc), and initial velocities such that at least the inner edge of the cloud is moving at less than the circular orbit speed. The required gravitational potential was essentially the same as that derived in § 4, assuming circular orbits.

Our principal doubts about models of this type involve the plausibility of the conditions required, particularly the steep dependence of drag on distance from the center. A medium in hydrostatic equilibrium with an adiabatic temperature gradient has a density varying approximately as $r^{-3/2}$. An isothermal medium could have a sufficiently steep density gradient, but it seems likely that the supersonic motion of clouds through the medium would result in higher temperatures near the center. Alternatively, drag could result from magnetic fields transferring angular momentum out to the molecular disk, rather than from motion through a medium. The initial condition of an extended cloud orbiting well within its Roche distance from the center also seems artificial; more realistic initial conditions might involve gradual feeding of gas into the spiral as the inner edge of the molecular is ionized.

An alternative model is suggested by the analogy to galactic spiral arms. Density wave theory predicts a spiral pattern can occur between the inner and outer Lindblad resonances in a rotating disk (e.g., Binney & Tremaine 1987). At these two radii, $\Omega_{\rm pat} = \Omega_{\rm orb} \pm \kappa/n$, where $\Omega_{\rm pat}$ is the pattern angular frequency, $\Omega_{\rm orb}$ is the orbital frequency, κ is the epicyclic frequency, and n is the number of spiral arms. Two-armed spirals dominate in a disk with a flat rotation curve. On the other hand, in a Keplerian disk $\kappa \approx \Omega_{\rm orb}$, and one-armed disturbances can propagate the entire way between the origin and the outer Lindblad resonance (Kato 1983; Adams, Ruden, &

Shu 1989). Because of the steep rotation curve of a Keplerian disk, two-armed disturbances can be maintained over only a small range in radius. Consequently, the observed one-armed spiral is the expected pattern for a density wave in the gravitational potential dominated by a point mass.

Outside of ~ 2 pc radius, the molecular disk has a roughly constant rotational speed, in which case a one-armed spiral cannot persist, and a two-armed disturbance would be expected. A two-armed spiral is not apparent in the molecular observations, but the discrepancies between the extrapolated spiral in the northeast (Fig. 3) are suggestive of the breakup of the one-armed pattern.

Several considerations suggest that the observed spiral may be driven by mechanisms different from those which drive normal galactic spiral arms. First, the stars in the inner few parsecs are not concentrated in a thin disk and have quite random orbits, so would not participate in a density wave. (They may, however, be in a somewhat flattened or barlike distribution, which could lead to noncircular gas motions.) Second, the gas disk is probably not sufficiently massive to be self-gravitating, suggesting that gravitational instabilities in the disk are not the driving mechanism. Alternatively, the magnetic fields present (Aitken et al. 1986, 1991; Hildebrand et al. 1990) may be capable of gathering the gas into the observed pattern. The best current magnetic field and gas density estimates indicate that magnetic forces are $\leq 10\%$ of gravitational forces, so comparable to the perturbations in gravitational forces which drive galactic spiral waves. Notably, Aitken et al. find that the magnetic field runs along the northern arm and into the bar, as we suggest the spiral does, and becomes disorganized just south of Sgr A*, where the fitted spiral turns toward the center.

It is also possible that the spiral is a region of enhanced ionization, rather than enhanced density. The region between the spiral wraps would then need to be filled with atomic gas (which is difficult to observe). In this case, a density wave shock would seem to be the most likely ionization mechanism, although the large required rate of kinetic energy loss by the orbiting gas may rule out this possibility (Lacy et al. 1980).

6. MASS DISTRIBUTION

The kinematics of the ionized gas along the spiral indicates that the gravitational field in the inner parsec of the Galaxy is dominated by a central mass concentration of $2 \pm 0.5 \times 10^6 M_\odot$ in addition to the distributed mass of an isothermal star cluster. Such a mass concentration has already been inferred from several previous studies. Our present study strengthens the argument for a massive object in two ways. First, we find that the gas moves on nearly circular orbits, ruling out any ejection model for its origin, and arguing strongly against dominance of any nongravitational forces, such as magnetic forces, which give no natural explanation for circular orbits or the nearly Keplerian rotation pattern. Any kinematic model which reproduces the nearly circular motion, whether it involves a density wave in a disk, a tidally stretched cloud, or another origin of the spiral, will require a mass concentration in addition to that of an isothermal star cluster to fit the increase in velocity toward the center. Second, we find that the central mass must be contained within a radius of less than 0.1 pc in order to fit the kinematics of the gas in the bar just south of Sgr A*. This is now a small enough radius to rule out the possibility of a stellar distribution sufficiently far from thermalized to mimic a central mass, as the thermalization time for a stellar mass of $2 \times 10^6 M_\odot$ within a 0.1 pc radius sphere is only $\sim 10^7$ yr, far less than the age of the Galaxy. We therefore conclude that there must be a $2 \times 10^6 M_\odot$ object, presumably a black hole, at the Galactic center.

We thank John Rawlins and John Feldmeier for assistance with the data reduction, K. Y. Lo and M. C. H. Wright for access to data, and K. Y. Lo, D. T. Jaffe, D. J. Hollenbach, and H. H. Coleman for helpful discussions. We also thank the staff of the IRTF for their assistance, especially J. Harwood and G. Koenig, who kept the scan capability available. This work was supported by the National Science Foundation and Texas Advanced Research Program.

REFERENCES

Adams, F. C., Ruden, S. P., & Shu, F. H. 1989, ApJ, 347, 959
Aitken, D. K., Gezari, D., Smith, C. H., McCaughrean, M., & Roche, P. F. 1991, ApJ, 380, 419
Aitken, D. K., Roche, P. F., Bailey, J. A., Briggs, G. P., Hough, J. H., & Thomas, J. A. 1986, MNRAS, 218, 363
Binney, J., & Tremaine, S. 1987, Galactic Dynamics (Princeton: Princeton Univ. Press)
Genzel, R., & Townes, C. H. 1987, ARA&A, 25, 377
Güsten, R., Genzel, R., Wright, M. C. H., Jaffe, D. T., Stutzki, J., & Harris, A. I. 1987, ApJ, 318, 124
Hildebrand, R. H., et al. 1990, ApJ, 362, 114
Jefferys, W., McArthur, B., & McCartney, J. 1990, BAAS, 22, 927
Kato, S. 1983, PASJ, 35, 249
Lacy, J. H. 1989, in IAU Symp. 136, The Center of the Galaxy, ed. M. Morris (Dordrecht: Kluwer), 493
Lacy, J. H., Achtermann, J. M., Bruce, D. E., Lester, D. F., Arens, J. F., & Gaalema, S. D. 1989, PASP, 101, 1166
Lacy, J. H., Townes, C. H., Geballe, T. R., & Hollenbach, D.J. 1980, ApJ, 241, 132
Lo, K. Y. 1989, in IAU Symp. 136, The Center of the Galaxy, ed. M. Morris, (Dordrecht: Kluwer), 527
Lo. K. Y., & Claussen, M. J. 1983, Nature, 306, 647
Lynden-Bell, D., & Rees, M. J. 1971, MNRAS, 152, 461
Mezger, P. J., & Wink, J. E. 1986, A&A, 157, 252
Morris, M., ed. 1989, IAU Symp. 136, The Center of the Galaxy (Dordrecht: Kluwer)
Quinn, P. J., & Sussman, G. J. 1985, ApJ, 288, 377
Rieke, G. H., & Rieke, M. J. 1988, ApJ, 330, L33
Roberts, D. A., Goss, W. M., van Gorkom, J. H., & Leahy, J. P. 1991, ApJ, 366, L15
Schwartz, U. J., Bregman, J. D., & van Gorkom, J. H. 1989, A&A, 215, 33
Sellgren, K., McGinn, M. T., Becklin, E. E., & Hall, D. N. B. 1990, ApJ, 359, 112
Serabyn, E., Güsten, R., Walmsley, C. M., Wink, J. E., & Zylka, R. 1986, A&A, 169, 85
Serabyn, E., & Lacy, J. H. 1985, ApJ, 293, 445
Serabyn, E., Lacy, J. H., Townes, C. H., & Bharat, R. 1988, ApJ, 326, 171
Sutton, E. C., Danchi, W. C., Jaminet, P. A., & Masson, C. R. 1990, ApJ, 384, 503
Wright, M. C. H., Genzel, R., Güsten, R., & Jaffe, D. T. 1987, in The Galactic Center, ed. D. C. Backer (AIP Conf. Proc. 155) (New York: AIP), 135